



## Research article

## Highly selective acetate production from wine lees through acidogenic fermentation

Alice Lanfranchi<sup>a,b,\*</sup>, Jose Antonio Magdalena<sup>a,c</sup>, Cristina Cavinato<sup>b</sup>, Eric Trably<sup>a</sup><sup>a</sup> INRAE, Univ Montpellier, LBE, 102 Avenue des Etangs, 11100 Narbonne, France<sup>b</sup> Dipartimento di Scienze Ambientali, Informatica e Statistica, Università Ca' Foscari Venezia, Mestre, 30172, Italy<sup>c</sup> Vicerrectorado de Investigación y Transferencia de la Universidad Complutense de Madrid, 28040, Madrid, Spain

## ARTICLE INFO

## Keywords:

Dark fermentation  
Winery waste  
Ethanol oxidation  
Chain elongation  
Microbial community

## ABSTRACT

Among winery wastes wine lees have a high, unexplored potential for the production of carboxylic acids and more particularly acetate. In fact, they have a high ethanol and low carbohydrate content which can make thermodynamically feasible the oxidation of ethanol to acetate. In this study, the potential of wine lees for anaerobic acetate production was assessed in batch conditions, 37 °C and pH 5.5. White wine lees (WWL) and red wine lees (RWL) were fermented with and without inoculum, and RWL were also co-fermented with waste activated sludge at 20, 40, 70 and 100 gCOD/L. Endogenous microbiome had the same fermentation performances than the external inoculum in WWL, while it led to almost no carboxylates production in RWL, where the community was dominated by the H<sub>2</sub>-producer *Klebsiella* (81.6%). Overall, acetate always represented the majority of carboxylates (58–72% on COD basis). H<sub>2</sub> production was low (0.31–6.97 mL H<sub>2</sub>/g bCOD<sub>in</sub>), thus enabling anaerobic ethanol oxidation to acetate ( $\Delta G = -26.6/-7.4$  kJ/mol). In co-fermentation, at 70 and 100 gCOD/L caproate (10.0–16.0%) and heptanoate (1.6–5.4%) appeared, alongside a microbiome enriched in lactate-producers (up to 24.5%). Overall, the high acetate selectivity obtained is promising for biorefinery process coupling.

## 1. Introduction

Today, global warming has already reached 1.1 °C and is predicted to attain at least 1.5 °C by 2040 and up to 4.4 °C by 2100 (IPCC, 2023). Greenhouse gases emissions are going to increase under the current system of production and consumption, concurrently with the environmental pollution caused by agricultural and industrial processes. A significant contribution to tackling this dual challenge can be brought by the environmental biorefinery, aiming at turning waste treatment into carbon neutral processes for resource and energy recovery.

Wine production is a large agro-industrial sector, with a production of 26 million m<sup>3</sup>/year generating 130 kg of pomace, 30 kg of stalks, 0.06 m<sup>3</sup> of wine lees and 1.65 m<sup>3</sup> of wastewaters from each ton of grapes (OIV, 2023; Oliveira and Duarte, 2016). In Europe, winery wastewaters are treated with the activated sludge process, thus contributing to the 6.1 million Mg of dry matter/year of waste activated sludge (WAS) generated in Europe, calculated with the most recent data (2019–2021) (Eurostat, 2023). Wine lees (WL) have a high BOD and COD demand which makes them harmful to the environment, and they usually

undergo ethanol distillation and tartaric acid recovery (Galanakis, 2017). However, ethanol distillation is a subsidized economic practice so, although this policy is environmentally sustainable, the development of a techno-economically feasible alternative would allow to achieve both the environmental and economic goals in winery waste management (Anderson and Jensen, 2018).

A promising alternative is winery waste treatment through anaerobic fermentation, a robust biological process able to convert a variety of organic wastes into energy (H<sub>2</sub>) and platform chemicals such as carboxylates and ethanol. Anaerobic fermentation is the first part of the anaerobic digestion process, where organic matter is converted into a CH<sub>4</sub>-rich biogas. Anaerobic fermentation consists of two subsequent phases with different end-products: i) dark fermentation (DF), yielding H<sub>2</sub> and carboxylates, and ii) acidogenic fermentation (AF), conducted until the acetogenic phase, where acetogens can oxidate the carboxylates into acetate and H<sub>2</sub> and homoacetogens can convert H<sub>2</sub> and CO<sub>2</sub> into acetate, thereby maximizing the carboxylates yield (Turon et al., 2016). With respect to the established aerobic acetic acid fermentation, the anaerobic one presents several advantages: i) in the perspective of

\* Corresponding author. Dipartimento di Scienze Ambientali, Informatica e Statistica, Università Ca' Foscari Venezia, Mestre, 30172, Italy.

E-mail addresses: [alanfra@outlook.it](mailto:alanfra@outlook.it), [alice.lanfranchi@unive.it](mailto:alice.lanfranchi@unive.it) (A. Lanfranchi).

<https://doi.org/10.1016/j.jenvman.2024.123532>

Received 22 July 2024; Received in revised form 18 October 2024; Accepted 27 November 2024

Available online 1 December 2024

0301-4797/© 2024 The Authors. Published by Elsevier Ltd. This is an open access article under the CC BY license (<http://creativecommons.org/licenses/by/4.0/>).

scale-up, it could entail lower costs since aeration is not required; ii) less biomass is produced, thereby potentially giving higher yields and a lower amount of solid to be treated at the end of the process; iii) the organic matter can be converted into other interesting fermentation products together with acetate, e.g.,  $H_2$ . The carboxylates-rich effluent can be directly used in subsequent biological processes, thus avoiding the energy-intensive carboxylates separation and purification, which accounts for 60–80% of the total production costs and entails product losses (Ragauskas et al., 2006; Ramos-Suarez et al., 2021; Rebecchi et al., 2016). Acetate is a target molecule to simply couple anaerobic fermentation with subsequent biological processes, since it is the most easily assimilable carboxylate by a variety of microorganisms such as microalgae or electroactive bacteria used in microbial electrolysis cells (MECs) (Lacroux et al., 2023; Magdalena et al., 2023; Marone et al., 2017). However, while the robustness of anaerobic fermentation is already established, it is still challenging to steer its selectivity towards specific products.

Among winery wastes Wine Lees (WL) have a high, unexplored potential for acetate production. They are mainly composed by dead yeast cells, polyphenols, tartrate salts and biodegradable compounds with high ethanol (87–122.0 g/L), and low carbohydrates (3.5–4.8%) concentrations (De Iseppi et al., 2020; Kucek et al., 2016). The concurrent high ethanol and low carbohydrates content can make ethanol oxidation (EEO) to acetate thermodynamically feasible. In fact, EEO is unfeasible under standard conditions ( $\Delta G^\circ = 9.6$  kJ/mol), but it becomes feasible at low partial pressures of  $H_2$  ( $p_{H_2} = 0.0003$ – $0.002$  bar), which are expected in the fermentation of substrates with a low carbohydrate content such as WL (Alibardi and Cossu, 2016; Roghair et al., 2018).

Given a substrate, pH and substrate concentration are among the most influential parameters in determining fermentation pathways, due to their influence on microbial activity and therefore substrate hydrolysis, fermentation rate,  $H_2$  production and carboxylates composition. The use of wine lees in anaerobic fermentation started attracting research interest only recently mainly for the production of medium chain carboxylates (MCCAs), while their potential for acetate production is still unexplored (Dessi et al., 2024; Kucek et al., 2016). However, some authors reported acetate production during the anaerobic fermentation of winery wastewater, which contains also wine lees. Information is generally lacking with respect to the effect of pH and substrate concentration on acetate selectivity in winery wastewater fermentation: in Vital-Jacome and Buitrón (2021), at pH 5.5, acetate selectivity was boosted to 100% by increasing the organic loading rate (OLR), while in Esteban-Gutiérrez et al. (2018) a 77% selectivity (COD basis) was reached in a batch alkaline fermentation at 10 gCOD/L. Moreover, the variability in the macromolecular and microbiological composition of winery wastewaters and inocula hinders the replicability of the studies. For instance, in comparable conditions (pH 5.5, 10 gCOD/L, mesophily, batch mode) Esteban-Gutiérrez et al. (2018) and Carrillo-Reyes et al. (2019) obtained different carboxylates profiles, mainly consisting of acetate (40%), propionate (42%) and butyrate (10%) for the former and acetate (29.5%), butyrate (34.5%), and iso-valerate (8.5%) for the latter.

In light of this, the novelty of this study relies in a systematic screening of the parameters steering the fermentation of WL towards acetate selectivity. This was done by investigating both biotic (endogenous and exogenous microbial community) and abiotic (substrate concentration and biochemical composition, micronutrients) parameters. First, two types of WL were fermented, with and without inoculum addition. In the perspective of process scale-up and applicability, red wine lees were then co-fermented with WAS at increasing substrate concentrations.

## 2. Materials and methods

### 2.1. Substrates characterization and inoculum

The substrates used in this study were WL and WAS. WL were generated by the vinification of red and white wine at the INRAE research unit of Pech Rouge (France) and are therein referred to as “red wine lees (RWL)” and “white wine lees (WWL)”. The samples of several vinification batches were collected to reach the necessary volume of WL. Then, they were homogenized and stored at  $-20$  °C. WAS was collected from the wastewater treatment plant (WWTP) of Narbonne (France), before the thickening stage. To reproduce a thickened WAS with 40 gTS/L at the moment of the experiments, it was centrifuged and the liquid and solid fractions were stored separately at  $-20$  °C. All the substrates were characterized respect to their total solids (TS), total volatile solids (TVS), total chemical oxygen demand (tCOD), soluble chemical oxygen demand (sCOD), biodegradable chemical oxygen demand (bCOD), carboxylates, ethanol, lactate, glycerol, proteins, carbohydrates, lipids, ammonium ( $NH_4^+$ ), phosphates ( $PO_4^{3-}$ ), nitrites ( $NO_2^-$ ), nitrates ( $NO_3^-$ ), pH, and conductivity.

The WAS collected at the WWTP of Narbonne was also used as inoculum, but for this use it was freeze-dried and stored at  $-80$  °C to preserve the microbial community and improve results reproducibility (Dauptain et al., 2021). The freeze-dried inoculum had a TVS content of 748.26 g/kg. Before fermentation, the inoculum was resuspended in water and pretreated at 90 °C for 15 min to eliminate non-spore forming microorganisms and select spore-forming  $H_2$ -producing bacteria (e.g. *Clostridium* sp.) (Argun and Kargi, 2009).

### 2.2. Acidogenic fermentation experiments

Fermentation was conducted in batch mode in 1L glass bottles of 0.5 L working volume with custom neck for sampling. Initial pH was set at 5.5 with NaOH 8M and was buffered with 400 mM MES (2-(N-morpholino)ethanesulfonic acid). The headspace of the bottles was flushed with  $N_2$  for 5 min before incubation at 37 °C. Mechanical stirring was performed before sampling. Each condition was tested in quadruplicate. Micronutrients were not added since they had no effect in the co-fermentation of WWL or RWL with WAS, where they were added to reach a concentration in the culture medium of (mg/L): 1.5 FeCl<sub>2</sub>, 0.06 H<sub>3</sub>BO<sub>3</sub>, 0.1 MnSO<sub>4</sub>, 0.025 CoCl<sub>2</sub>, 0.070 ZnCl<sub>2</sub>, 0.025 NiCl<sub>2</sub>, 0.015 CuCl<sub>2</sub>, 0.025 Na<sub>2</sub>MoO<sub>4</sub> (Table S1). Therefore, the complex substrates used already contained all the necessary micronutrients for the microorganisms involved in dark fermentation, and in particular Fe and Ni, which are required for the synthesis of the hydrogenases (Bardi et al., 2023; Hallenbeck, 2009).

Two types of experiments were conducted. Fermentation of RWL and WWL was conducted with and without inoculum at a substrate concentration of 20 gCOD/L. This test lasted 9 days. A pseudo steady-state was reached from day 7, which was therefore kept as end day for the subsequent tests. Test duration was set to target acetate production, occurring in the first days. Acidogenic co-fermentation of RWL and WAS was conducted at increasing substrates concentrations of 20, 40, 70 and 100 gCOD/L with a 4:1 ratio on a COD basis, representing the real waste fluxes of a winemaking company located in North-eastern Italy (Da Ros et al., 2017).

10 mL of effluent were sampled daily for carboxylates, pH and microbial community analyses. Gas production and composition were monitored online every 2h with a micro-gas chromatograph (MicroGC, SRA I-GC R3000). The content in ethanol, lactate, glycerol and 1,3-propanediol was monitored at the beginning and end of the experiment.

### 2.3. Analytical methods

TS and VS were determined based on the method proposed by Kreuger et al. (2011) to correct for the losses in volatile compounds such

as ethanol during drying at 105 °C. tCOD and sCOD were measured with commercial kits (Lovibond, Germany). bCOD of the solid fraction was determined by assessing the biochemical methane potential through near-infrared spectroscopy (Flash BMP®) and then applying the theoretical conversion factor of 350 mL CH<sub>4</sub>/g bCOD and relating it to the TVS content of the substrates. bCOD of the liquid fraction was calculated considering that the biodegradable organic molecules present in the liquid phase represented all the biodegradable compounds contained therein, as indicated by the COD<sub>analytes</sub>/sCOD of 1. NH<sub>4</sub><sup>+</sup>, PO<sub>4</sub><sup>3-</sup>, NO<sub>2</sub><sup>-</sup> and NO<sub>3</sub><sup>-</sup> were determined colorimetrically with the Gallery™ sequential analyser (Thermo Scientific). Protein content was determined by multiplying Total Kjeldahl Nitrogen for the conversion factor of 6.25 g proteins/g N, *i.e.*, under the assumption that proteins contain 16.5% (w/w) of nitrogen (Raunkjer et al., 1994). Carbohydrates were determined with the anthrone method (Dreywood, 1946). pH was measured with a Five Easy™ pHmeter (Mettler Toledo) and conductivity with a WTW Multi 3410 IDS conductimeter. The concentrations of carboxylates were determined daily on the supernatant filtered with nylon filters with a pore size of 0.2 µm after centrifugation at 12,000 rpm for 5 min. The analysis was conducted with a Clarus 580 gas-chromatograph (PerkinElmer, Waltham, MA, USA) equipped with a AlltechFFAP EC™ 1000 column and a flame ionization detector (FID) at 280 °C, with N<sub>2</sub> as carrier gas (6 mL/min). Ethanol, lactate, glycerol and 1,3-propanediol were monitored by High-Performance Liquid Chromatography (HPLC) with a Dionex Ultimate 3000 (ThermoScientific) equipped with a protective pre-column (Bio-Rad Micro-Guard Cation H+), an Aminex HPX-87H Ion exclusion column and a refractive index detector (ERC RefractoMax 520). The analysis was conducted at 50 °C, with 0.04 M H<sub>2</sub>SO<sub>4</sub> at a flow of 0.6 mL/min as eluent.

#### 2.4. Calculations

The yield indicates the amount of bCOD of the substrates converted into fermentative metabolites. For the liquid products (carboxylates and 1,3-propanediol), yield was calculated as it follows (Eq. (1)):

$$\text{Yield} \frac{\text{gCOD}_{\text{prod}}}{\text{g bCOD}} = \frac{\text{Products concentration} \left( \frac{\text{gCOD}}{\text{L}} \right) \times \text{working volume (L)}}{\text{Substrates' concentration} \left( \frac{\text{g bCOD}}{\text{kg}} \right) \times \text{substrates inserted (kg)}} \quad (1)$$

Where working volume was the real working volume, considering samples withdrawal.

For the gaseous products, yield was calculated as mL gas/g bCOD inserted. The volume of gas produced was calculated through the pressure variations, as detailed in Roslan et al. (2023). Carboxylates selectivity was expressed as a percentage on a COD basis of the total carboxylates produced.

Thermodynamic calculations were performed as in Kleerebezem and Van Loosdrecht (2010) using their  $\Delta G_f^0$  and  $H_f^0$  values. The missing  $H_f^0$  values were retrieved from the OBGIT thermodynamic database in the R package CHNOSZ. Temperature corrections to 37 °C to the standard variation in Gibbs free energy ( $\Delta G^0$ ) were made by applying the Gibbs-Helmholtz equation.

The mass balance was conducted to elucidate the metabolic pathways involved in ethanol consumption and acetate production. To do so, it was assumed that butyrate, valerate, caproate and heptanoate were produced by chain elongation using ethanol as electron donor. Then, the rest of the consumed ethanol was considered to be converted into acetate by EEO. The acetate produced and consumed in chain elongation was also accounted for. The part of the acetate measured that was not produced from EEO was assumed to be produced by the primary fermentation of the substrates, since homoacetogenesis was probably hindered by the low p<sub>H<sub>2</sub></sub> (<0.04 bar) and high acetate concentrations (>10 mM) (Bastidas-Oyanedel et al., 2012).

#### 2.5. Sequencing and microbial community analysis

The biomass pellet obtained after centrifugation was used for microbiological analyses. DNA extraction was performed with the FastDNA SPIN kit for soil following manufacturer's instructions (MP biomedical, LCC, California, USA). The V3-V4 region of the 16S rRNA gene was amplified by PCR using universal primers (Carmona-Martínez et al., 2015). The PCR mix was composed of iproof (Biorad, 0,02U/µl) with enzyme buffer, forward (344F: ACGGRAGGAGCAG) and reverse (802R: TACCAGGGTATCTAATCCT) primers (0.5 mM), dNTP (0.2 mM), sample DNA (5–10 ng/µL) and water until reaching a final volume of 50 µL. 30 cycles of denaturation (95 °C, 1 min), annealing (65 °C, 1 min) and elongation (72 °C, 1 min) were conducted in a thermal cycler (Mastecycler, Eppendorf, Germany). A final extension step was added for 10 min at 72 °C after the 30 amplification cycles. PCR amplifications were verified by 2100 Bioanalyzer (Agilent, USA). Amplicons were sequenced at the GenoToul platform (Toulouse, France <http://www.genotoul.fr>) using an Illumina Miseq sequencer (2 × 300 pb paired-end run). Raw sequences were then analyzed with Mothur version 1.48.0 for reads cleaning, assembly, and quality checking. Alignment and taxonomic outlines were obtained from SILVA release 132. Sequences were archived in GenBank, under the accession number PRJNA1028514. The rRNA sequences of OTUs with relative abundance ≥1% were then submitted to Megablast to search within the NCBI nucleotide database.

Bioinformatic analyses were conducted in R version 4.3.1 with the packages *phyloseq*, *microbiome*, *vegan*, *MicEco*, *microeco*. Graphs were realized with *ggplot2*, *fantaxtic* and *ggnested* (Teunisse, 2022). Spearman's correlation between the environmental variables and the OTUs was calculated with the *trans\$env* function in the *microeco* package. To evaluate the distance between samples, Principal Coordinates Analysis (PCoA) was performed with the *capscale* function in the *vegan* package. The correlation between microbiome composition and environmental factors was investigated by fitting the PCoA scores with the *envfit* *vegan* function.

#### 2.6. Statistical analyses

Statistical analyses were conducted in R version 4.3.1 with the *stats* package. The differences among all the conditions tested were evaluated with the Kruskal-Wallis test. For comparing two conditions, the Mann-Whitney-Wilcoxon test was applied. The level of significance was set at  $p < 0.05$ .

### 3. Results and discussion

#### 3.1. Substrates characterization

Overall, the characteristics of the substrates reported in Table 1 were coherent with those reported in literature, considering that Wine Lees (WL) have a heterogeneous composition, varying widely depending on the types of grapes and yeasts used and on the vinification process. Specifically, pH was ~4 and TS content was comprised between 12.3 and 163.7 g/kg, as reported elsewhere (Bustamante et al., 2008; Da Ros et al., 2017; Jasko et al., 2012). Conductivity (2.22–2.49 mS/cm) was slightly lower than in literature (4.0–13.8 mS/cm), but this could not be related to the content in NH<sub>4</sub><sup>+</sup> and PO<sub>4</sub><sup>3-</sup> since these values were not reported (Bordiga, 2016). White Wine Lees (WWL) showed a lower TS content of 75.4 g/kg and a higher ethanol concentration of 122.00 g/L respect to Red Wine Lees (RWL), since more wine was necessary to remove WWL from the vinification reactor. Both RWL and WWL contained glycerol (9.85–7.07 g/L) and acetate in minor concentrations (0.51–0.24 g/L), which are among the hundreds of by-products generated by ethanol fermentation, precisely through the concomitant pathway of glycerol-pyruvic fermentation (Ciani et al., 2018). RWL also contained lactate, produced by malo-lactic fermentation, where lactic

**Table 1**  
Substrates characteristics.

PARAMETER	UNIT	RWL	WWL	WAS	CONCENTRATED WAS
pH		4.15 ± 0.05	4.09 ± 0.05	7.30 ± 0.04	7.29 ± 0.04
Conductivity	mS/cm	2.49 ± 0.01	2.22 ± 0.01	1.42 ± 0.01	1.42 ± 0.01
TS	g/kg	129.4 ± 0.05	75.4 ± 0.4	5.5 ± 0.0	40.0 ± 0.0
VS		116.6 ± 0.6	63.0 ± 0.2	3.9 ± 0.0	31.1 ± 0.0
TS (corrected)		242.1 ± 0.5	207.2 ± 0.4	–	–
VS (corrected)		229.3 ± 0.6	194.7 ± 0.2	–	–
Acetic acid	g/L	0.51	0.24	0.00	0.00
Lactate		1.90	0.00	0.00	0.00
Glycerol		9.85	7.07	0.00	0.00
Ethanol		107.29	122.00	0.00	0.00
sCOD	g/L	228.17 ± 5.04	254.50 ± 2.59	0.02 ± 0.00	0.02 ± 0.00
COD <sub>analytes</sub> /sCOD	g/g	1.04	1.08	–	–
tCOD	g/L	353.33 ± 6.62	296.17 ± 3.66	7.93 ± 0.27	50.19 ± 0.27
Flash BMP (solid)	mL CH <sub>4</sub> /gVS	229.23 ± 4.23	217.95 ± 3.44	202.15 ± 2.15	202.15 ± 2.15
Biodegradable COD	g bCOD/kg raw	283.7 ± 1.4	294.2 ± 0.6	2.2 ± 0.0	18.0 ± 0.2
	g bCOD/g COD	0.803	0.993	0.322	0.358
	g bCOD/g VS	1.237	1.511	0.578	0.578
TKN (solid)	g N/kgTS	43.60 ± 0.07	45.77 ± 0.32	62.28 ± 6.42	62.28 ± 6.42
Proteins	g/kgTS	272.49 ± 0.07	286.07 ± 0.32	389.25 ± 6.42	389.25 ± 6.42
Carbohydrates		43.09 ± 1.29	52.12 ± 3.25	30.57 ± 6.64	30.57 ± 6.64
NH <sub>4</sub> <sup>+</sup>	mg/L	3.9 ± 0.2	19.5 ± 0.9	18.9 ± 0.9	18.9 ± 0.9
PO <sub>4</sub> <sup>3-</sup>		497.4 ± 4.4	600.5 ± 1.4	154.0 ± 0.0	154.0 ± 0.0
NO <sub>3</sub> <sup>-</sup>		3.55 ± 0.2	1.88 ± 0.1	3.37 ± 0.2	3.37 ± 0.2

bacteria convert the tart-tasting malic acid, naturally contained in grape must, into softer-tasting lactic acid. Malo-lactic fermentation is not performed in white wines, and therefore this compound was not detected in WWL. Respect to their macromolecular composition, RWL and WWL were composed by a low percentage of carbohydrates (4.3–5.2% of TS) and by a considerable percentage of proteins (27.5–28.6% of TS), respectively similar (3.5–4.8%) and higher (14.5–15.7%) than those reported in literature (Bordiga, 2016). Considering protein content to be mainly due to yeast cells, which are composed by ~40% of proteins, it can be estimated that yeasts constituted 68–71.5% of the TS in RWL and WWL, respectively (Yamada and Sgarbieri, 2005). The difference probably consisted of tartrate salts, polyphenols, the fraction of glycerol which did not evaporate and other minor unidentified compounds. The bCOD of WWL and RWL represented 99.3% and 80.3% of the tCOD, respectively, with the higher biodegradability of WWL attributable to its higher ethanol and lower TS content. Regarding Waste Activated Sludge (WAS), its low TS concentration was coherent with the fact that it was unthickened. The content in proteins and carbohydrates was calculated with the conversion factors reported in Ahnert et al. (2021) and Miron et al. (2000) and it was comparable with literature, representing 38.9% and 3.06% of the TS and 49.7% and 2.7% of the tCOD, respectively (Chen et al., 2007). Concentrated WAS refers to the same WAS which was prepared at a TS concentration of 40 g/L for the fermentation experiments. Therefore, it had the same characteristics of WAS, except a higher TS, VS, and COD concentration.

Thorough substrate characterization allowed to make hypothesis on substrate conversion pathways during fermentation: in fact, a low H<sub>2</sub> production was expected with a low carbohydrate content, and the presence of ethanol could determine acetate production through EEO or caproate and heptanoate production through chain elongation (Alibardi and Cossu, 2016; Roghair et al., 2018).

### 3.2. Acidogenic fermentation experiments

In the first fermentation experiment conducted on WWL and RWL, with and without inoculum, the fermentation performance varied but acetate always represented the majority of the carboxylates

(61.0–71.8% on a COD basis) (Table 2). The pH remained approximately stable, with final values of 5.58–5.86. WWL had similar yields of 0.134 and 0.131 g COD<sub>prod</sub>/g bCOD with and without inoculum, respectively ( $p = 0.7715$ ). The H<sub>2</sub> yield was very low and also similar, showing a higher variability without inoculum ( $0.31 \pm 0.09$  and  $1.73 \pm 1.66$  mL H<sub>2</sub>/g bCOD with and without inoculum, respectively;  $p = 0.2845$ ). The carboxylates profile was similar, and it mainly consisted of acetate (61.0–65.7%), with minor amounts of caproate produced only without inoculum (6.5%, 0.17 g COD/L). This was probably due to the lower butyrate concentration (0.20 vs 0.44 g COD/L), attributable in turn to the lower relative abundance of *Clostridiaceae* (11.02 vs 19.72%), which could perform chain elongation of acetate to butyrate (section 3.4) (Candry and Ganigué, 2021, and references therein). RWL showed almost no carboxylates production without inoculum (0.058 g COD<sub>prod</sub>/g bCOD), while a yield of 0.232 g COD<sub>prod</sub>/g bCOD was reached with inoculum, where acetate (71.8%) and butyrate (21.6%) were the main carboxylates produced. Interestingly, the H<sub>2</sub> yield was similar, with values of 6.90 and 6.97 mL H<sub>2</sub>/g bCOD with and without inoculum, respectively. This can be explained by the differences in microbial communities after the H<sub>2</sub> production phase, as discussed in detail in section 3.4. Overall, inoculation ameliorated the fermentation performances in RWL, while no improvement was observed in WWL. The lower H<sub>2</sub> yield of WWL respect to RWL could be attributed to the lower TS content (75.4 vs 129.4 gTS/kg) and higher ethanol content of WWL, which determined a lower input of carbohydrates (4.3–5.2% on a TS basis) in the bottle for the same amount of COD. Moreover, the lower initial ethanol content in RWL (~4.9 g/L) with respect to WWL (~7.4 g/L) could have favored higher H<sub>2</sub>-yielding microorganisms (section 3.4). Hydrogen consumption through homoacetogenesis was considered unlikely to occur, given the low p<sub>H<sub>2</sub></sub> (<0.04 bar) and high acetate concentrations (>10 mM) measured in the bottles which were reported to hinder this reaction (Bastidas-Oyanedel et al., 2012).

Acetate was the main product also during the co-fermentation of RWL and WAS at 20, 40, 70, and 100 gCOD/L, as it represented 68.0, 72.3, 67.7, and 57.5% of the carboxylates on a COD basis, respectively. The pH remained approximately stable, with final values of 5.27–5.68. As illustrated in Fig. 1, the increase in substrate concentration determined a wider carboxylates distribution on day 7 at 70 and 100 gCOD/L,

**Table 2**

Carboxylates percentages, products concentrations and yields, and ethanol removal on day 7 and H<sub>2</sub> and CO<sub>2</sub> yields and percentages in the produced biogas at the end of the acidogenic fermentation phase (~ day 2). \* = test closed on day 4.

Parameter	Unit	WWL	WWL + inoc	RWL	RWL + inoc	RWL + WAS			
						20*	40	70	100
<b>Acetate</b>	% (COD basis)	<b>61.0 ± 5.5</b>	<b>65.7 ± 7.7</b>	<b>61.6 ± 19.0</b>	<b>71.8 ± 4.2</b>	<b>68.0 ± 2.3</b>	<b>72.3 ± 8.0</b>	<b>67.7 ± 1.7</b>	<b>57.5 ± 1.0</b>
Propionate		7.3 ± 7.7	14.7 ± 15.2	0.7 ± 0.5	0.9 ± 0.5	12.0 ± 0.2	7.3 ± 0.2	3.2 ± 0.2	2.6 ± 0.1
Iso-butyrate		2.1 ± 0.4	3.4 ± 0.5	2.7 ± 0.6	1.9 ± 1.1	1.2 ± 0.2	1.3 ± 0.2	1.6 ± 0.0	1.8 ± 0.0
Butyrate		16.2 ± 2.0	7.4 ± 2.2	29.9 ± 5.6	21.6 ± 2.7	15.3 ± 0.7	14.1 ± 1.3	9.4 ± 0.3	9.0 ± 0.2
Iso-valerate		5.6 ± 1.2	5.6 ± 0.2	5.1 ± 1.2	2.1 ± 0.2	1.9 ± 0.2	2.1 ± 0.3	2.7 ± 0.1	3.5 ± 0.1
Valerate		1.3 ± 1.8	0.4 ± 0.7	0.0 ± 0.0	0.0 ± 0.0	1.5 ± 0.3	1.8 ± 0.3	3.5 ± 0.3	4.2 ± 0.1
Iso-caproate		0.0 ± 0.0	3.0 ± 0.3	0.0 ± 0.0	0.0 ± 0.0	0.0 ± 0.0	0.0 ± 0.0	0.5 ± 0.0	0.0 ± 0.1
Caproate		6.5 ± 2.0	0.0 ± 0.0	0.0 ± 0.0	1.7 ± 2.0	0.0 ± 0.0	1.2 ± 0.5	10.0 ± 2.3	16.0 ± 0.9
Heptanoate		0.0 ± 0.0	0.0 ± 0.0	0.0 ± 0.0	0.0 ± 0.0	0.0 ± 0.0	0.0 ± 0.0	1.6 ± 1.2	5.4 ± 0.5
Acetate	gCOD/L	1.66 ± 0.29	1.80 ± 0.21	0.54 ± 0.17	2.63 ± 0.16	2.18 ± 0.07	5.53 ± 0.61	9.09 ± 0.23	10.42 ± 0.18
Propionate		0.24 ± 0.28	0.40 ± 0.42	0.01 ± 0.00	0.03 ± 0.02	0.39 ± 0.01	0.55 ± 0.01	0.43 ± 0.03	0.47 ± 0.02
Iso-butyrate		0.06 ± 0.00	0.09 ± 0.01	0.02 ± 0.01	0.07 ± 0.04	0.04 ± 0.00	0.10 ± 0.01	0.21 ± 0.01	0.33 ± 0.01
Butyrate		0.44 ± 0.06	0.20 ± 0.06	0.26 ± 0.05	0.79 ± 0.10	0.49 ± 0.02	1.08 ± 0.10	1.26 ± 0.04	1.62 ± 0.04
Iso-valerate		0.15 ± 0.01	0.15 ± 0.01	0.04 ± 0.01	0.08 ± 0.01	0.06 ± 0.01	0.16 ± 0.02	0.36 ± 0.01	0.63 ± 0.01
Valerate		0.04 ± 0.06	0.01 ± 0.02	0.00 ± 0.00	0.00 ± 0.00	0.05 ± 0.01	0.13 ± 0.02	0.47 ± 0.04	0.76 ± 0.02
Iso-caproate		0.00 ± 0.00	0.08 ± 0.01	0.00 ± 0.00	0.00 ± 0.00	0.00 ± 0.00	0.00 ± 0.00	0.06 ± 0.01	0.01 ± 0.02
Caproate		0.17 ± 0.04	0.00 ± 0.00	0.00 ± 0.00	0.06 ± 0.07	0.00 ± 0.00	0.09 ± 0.04	<b>1.34 ± 0.31</b>	<b>2.90 ± 0.17</b>
Heptanoate		0.00 ± 0.00	0.00 ± 0.00	0.00 ± 0.00	0.00 ± 0.00	0.00 ± 0.00	0.00 ± 0.00	<b>0.21 ± 0.16</b>	<b>0.98 ± 0.09</b>
Total carboxylates		2.76 ± 0.50	2.75 ± 0.23	0.88 ± 0.15	3.67 ± 0.25	3.21 ± 0.08	7.65 ± 0.57	13.43 ± 0.27	18.14 ± 0.26
1,3-PDO		0.24 ± 0.27	0.34 ± 0.24	0.24 ± 0.29	0.56 ± 0.03	0.52 ± 0.03	1.03 ± 0.09	1.41 ± 0.04	2.07 ± 0.03
<b>Yield</b>	<b>gCOD<sub>prod</sub>/gbcOD</b>	<b>0.131 ± 0.040</b>	<b>0.134 ± 0.024</b>	<b>0.058 ± 0.017</b>	<b>0.232 ± 0.018</b>	<b>0.230 ± 0.010</b>	<b>0.269 ± 0.022</b>	<b>0.266 ± 0.009</b>	<b>0.244 ± 0.007</b>
	gCOD <sub>carboxylates</sub> /gbcOD	0.122 ± 0.029	0.120 ± 0.016	0.048 ± 0.008	0.200 ± 0.019	0.201 ± 0.006	0.237 ± 0.019	0.240 ± 0.009	0.219 ± 0.007
	gCOD <sub>prod</sub> /gCOD	0.131 ± 0.040	0.134 ± 0.024	0.044 ± 0.012	0.204 ± 0.037	0.167 ± 0.005	0.191 ± 0.091	0.189 ± 0.007	0.174 ± 0.005
H <sub>2</sub> yield	mLH <sub>2</sub> /gbcOD	1.73 ± 1.66	0.31 ± 0.09	6.97 ± 2.06	6.90 ± 1.02	0.99 ± 0.12	1.46 ± 0.17	2.86 ± 0.24	1.96 ± 0.09
CO <sub>2</sub> yield	mLCO <sub>2</sub> /gbcOD	7.93 ± 3.46	7.44 ± 0.12	15.49 ± 2.55	16.53 ± 1.91	8.89 ± 1.71	14.20 ± 1.90	19.51 ± 1.55	20.62 ± 0.73
H <sub>2</sub>	%	22.9 ± 1.1	4.0 ± 1.1	30.5 ± 3.2	29.4 ± 2.2	10.6 ± 1.8	9.4 ± 0.9	12.8 ± 0.3	8.7 ± 0.5
CO <sub>2</sub>	%	77.1 ± 6.6	96.0 ± 1.1	69.5 ± 3.2	70.6 ± 2.2	89.4 ± 1.8	90.6 ± 0.9	87.2 ± 0.3	91.3 ± 0.5
Initial ethanol concentration	g/L	7.38 ± 0.03	7.35 ± 0.18	4.89 ± 0.09	4.90 ± 0.09	4.44 ± 0.03	8.82 ± 0.10	14.79 ± 0.32	22.14 ± 0.73
Final ethanol concentration		6.54 ± 0.21	6.72 ± 0.09	5.17 ± 0.10	3.63 ± 0.22	3.51 ± 0.03	6.32 ± 0.23	10.13 ± 0.28	15.47 ± 0.13
<b>Ethanol removal</b>	<b>%</b>	<b>11.3 ± 3.1</b>	<b>8.5 ± 2.1</b>	<b>5.7 ± 3.6</b>	<b>26.3 ± 3.6</b>	<b>20.9 ± 0.7</b>	<b>28.4 ± 3.4</b>	<b>31.5 ± 1.7</b>	<b>30.1 ± 2.2</b>

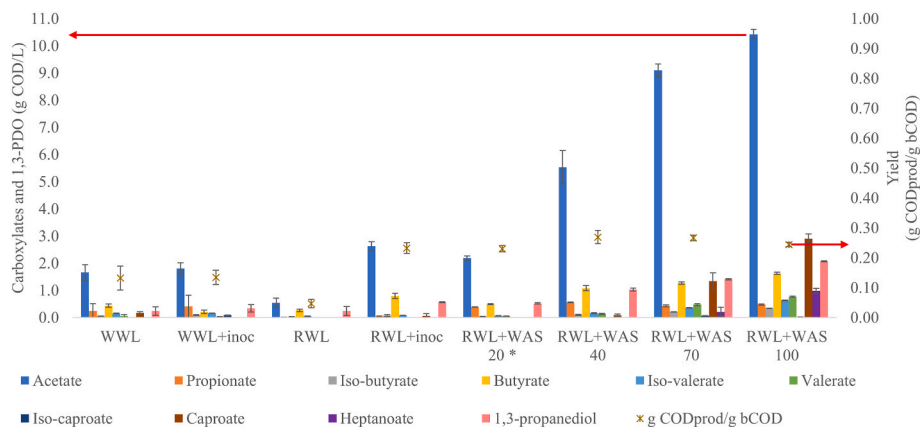


**Fig. 1.** Carboxylates and 1,3-PDO concentrations and product yield on day 7. The red arrows indicate the scale at which the data should be read. \* = test closed on day 4. (For interpretation of the references to color in this figure legend, the reader is referred to the Web version of this article.)

with the increase in valerate (3.5–4.2%) and the appearance of caproate (10.0 and 16.0%) and heptanoate (1.6–5.4%) (Table 2). Concurrently, lower percentages of propionate and butyrate were observed on day 7 (3.2–2.6% of propionate, 9.4–9.0% of butyrate) with respect to day 4 (8.5–9.0% of propionate and 14.6–15.8% of butyrate) at 70 and 100 gCOD/L, respectively (Fig. S1). At 100 gCOD/L, also the percentage of

acetate was statistically significantly lower (57.5%,  $p = 0.00473$ ). This can be explained by the occurrence of chain elongation, a secondary fermentation process where the carboxylic acid chain is elongated through sequential additions of two atoms of carbon, using ethanol and/or lactate as electron donors. Therefore, acetate was probably elongated to butyrate and then caproate, and propionate to valerate and then

heptanoate. The occurrence of chain elongation was supported also by the microbial community composition, where the butyrate-producer *Eubacteriales Family XIII* and the lactate-producers *Enterococcaceae*, *Lactobacillaceae*, and *Coriobacteriaceae* increased their relative abundance (section 3.4). The H<sub>2</sub> yield was very low in all the substrate concentrations tested, ranging from 0.99 to 2.86 mL H<sub>2</sub>/g bCOD. The product yields were similar (0.230–0.269 g COD<sub>prod</sub>/g bCOD), suggesting that the increase in ethanol concentration did not have an inhibitory effect. No inhibition could be attributed to the conductivity of the substrates (1.42–2.49 mS/cm), which even without dilution was lower than the inhibitory thresholds of 55 ± 4 and 46 ± 3 mS/cm identified for H<sub>2</sub> and carboxylates production, respectively (Trably et al., 2017). Similarly, at 20 g COD/L acetate and butyrate concentrations were below the inhibitory threshold of 50 mM for H<sub>2</sub> production (Noguer et al., 2022). Therefore, the low yields observed are attributable to a lower substrate mobilization at pH 5.5 by the microbial communities, especially the ones of inoculum and WAS which were adapted to pH ~7.0. Yields could be enhanced by adapting the microbial community at pH 5.5 in a continuous process, and by pre-treating the substrate to destroy the cellular wall of the yeasts and bacteria which mainly constitute WL and WAS. This would enhance the availability of the nutrients contained in the yeast cells (e.g. amino acids and peptides), which are known to promote microbial growth (Pérez-Bibbins et al., 2015).

Overall, acetate was the main carboxylate produced in all conditions, with a high selectivity of 57.5–72.3% on a COD basis, and a low H<sub>2</sub> yield was observed, ranging from 0.99 to 6.97 mL H<sub>2</sub>/g bCOD (Table 2). These results were consistent with the biochemical composition of the substrates: in fact, the low carbohydrate content (4.3–5.2% of the TS) explained the low H<sub>2</sub> production obtained, which in turn determined a pH<sub>2</sub> low enough to allow EEO to occur ( $\Delta G = -26.6/-7.4$  kJ/mol) (Alibardi and Cossu, 2016). As detailed in the mass balance (section 3.3), acetate was mainly produced by EEO, while a lower percentage derived from the primary fermentation of the substrates (0.0–34.4%). This is coherent with acetate being reported as the main carboxylate produced in the anaerobic fermentation of WAS (Jankowska et al., 2015).

The acetate selectivity obtained is among the highest in literature on organic substrates. On food waste, Cheah et al. (2019) reported a higher selectivity of ~85% on a COD basis (calculated) with a yield of ~0.35 g<sub>carboxylates</sub>/gVS, at pH 9.0 and at OLR of ~17.5 gVS/L\*d. Despite the higher acetate selectivity, the yield was lower than in our experiments, where 0.42–0.50 g<sub>carboxylates</sub>/gVS (corrected) were obtained during the co-fermentation of RWL and WAS. On winery wastewater, which is also composed of wine lees, Esteban-Gutiérrez et al. (2018) obtained a slightly higher acetate selectivity (77% on a COD basis) in batch at pH 10 and 10 gCOD/L, with a yield of 0.26 gCOD<sub>carboxylates</sub>/gCOD. In contrast with our results, they obtained a lower acetate percentage (40%) at pH 5.5, with a profile composed of propionate (42%) and butyrate (10%) (Esteban-Gutiérrez et al., 2018). Similarly, a lower acetate percentage (29.5%) on winery wastewaters at pH 5.5 and 10 gCOD/L was also reported by Carrillo-Reyes et al. (2019), with a yield of 0.30 gCOD<sub>carboxylates</sub>/gCOD. Here, the carboxylates profile was composed of butyrate (34.5%), iso-valerate (8.5%), propionate (7%), iso-butyrate (6.3%) and valerate (5.3%).

Interestingly, in our study acidic conditions gave a high acetate selectivity, which on winery wastewaters was observed only in alkaline conditions with comparable yields (Esteban-Gutiérrez et al., 2018). This could be attributed to the higher ethanol content (107.3–122.0 g/L) and lower carbohydrate content (3.9–5.6 g/L) of the WL used in this study with respect to winery wastewaters (56.1–73.9 and 26.9–32.9 g/L), which favored EEO to acetate (Carrillo-Reyes et al. (2019); Vital-Jacome and Buitrón, 2021). The lower carbohydrate content could also explain the lower yields obtained (0.167–0.204 gCOD<sub>prod</sub>/gCOD) with respect to Carrillo-Reyes et al. (2019) and Esteban-Gutiérrez et al. (2018) (0.30 and 0.26 gCOD<sub>carboxylates</sub>/gCOD, respectively).

The low yields and ethanol removal obtained are the main limitations of the process presented in this work, which could be enhanced by i) adapting the microbial community to pH 5.5 by operating the process in continuous and ii) pre-treating the substrate to destroy the cellular wall of the yeasts and bacteria which mainly constitute the substrates. The increase in ethanol consumption could eventually enhance acetate selectivity if EEO remains the prevailing pathway.

### 3.3. Mass balance

The mass balance was conducted to elucidate the metabolic pathways underlying ethanol consumption and acetate production. To do so, butyrate, valerate, caproate and heptanoate were considered to be produced by chain elongation using ethanol as electron donor. Then, it was considered that the rest of the ethanol consumed in the experiment was converted into acetate by EEO. The acetate produced and consumed in chain elongation was also accounted for. The part of the acetate measured that was not produced from EEO was assumed to be produced by the primary fermentation of the substrates, since homoacetogenesis was probably hindered by the low pH<sub>2</sub> (<0.04 bar) and high acetate concentrations (>10 mM) (Bastidas-Oyanedel et al., 2012).

The results of the mass balance are presented in Table 3. In all the conditions tested except RWL, the ethanol consumed was mainly converted into acetate by EEO (76.2–95.0%). This was supported by the  $\Delta G$  values for EEO, which was thermodynamically feasible under the tested experimental conditions ( $\Delta G = -26.6/-7.4$  kJ/mol). A lower percentage of ethanol was consumed in chain elongation (5.0–23.8%). Acetate was mainly produced from ethanol oxidation (65.6–115.5%), with a lower percentage deriving from the primary fermentation of the substrates (0.0–34.4%). Under the assumption that the acetate not produced by EEO was produced by the primary fermentation of the substrates, all the mass balances except that of WWL were closed with an error <3.4%. In RWL, ethanol consumption (5.7%) and carboxylates production were minimal (0.54 and 0.26 gCOD/L of acetate and butyrate, respectively), thus explaining the different repartition of the ethanol consumed and acetate produced with respect to the other conditions. Overall, the mass balance indicated that EEO was the prevailing fermentation pathway, through which most of the acetate was produced.

### 3.4. Microbial communities

Microbial communities were analyzed by sequencing the V3-V4 region of the 16S rRNA gene on the substrates and inoculum and on the fermented samples at day 7 for all conditions, except RWL + WAS 20 which was sampled at day 4. In the substrates and inoculum 1181 OTUs were identified, which were grouped into 27 phyla, 62 classes, 136 orders, 281 families, and 613 genera. After filtering at 1% of relative abundance, 11 orders, 13 families and 18 genera were kept. In the fermented samples, 997 OTUs were identified, which were grouped into 22 phyla, 45 classes, 96 orders, 183 families, and 356 genera. After filtering at 1% of relative abundance, 5 orders, 9 families and 15 genera were kept. The 12 most abundant orders and two most abundant families for each order in all the samples are represented in Fig. 2, while the tables reporting the relative abundance and closest species match of all the taxa after filtering at 1% can be consulted in the Supplementary Materials (Tables S2 and S3).

In the substrates, a higher richness was observed in white wine lees (231) with respect to red wine lees (60), which could have played a role in the higher products yield of white wine lees when fermented without inoculation (Table 4). White wine lees had lower Shannon's diversity and evenness (2.69 and 0.494) with respect to red wine lees (3.23 and 0.070), due to the high relative abundance of OTU 14 of the *Erwinaceae* family (43.87%), which had 99.06% similarity to *Tatumella saanichensis*. *Tatumella* spp. belong to the *Enterobacteriales* order, one of the most abundant in wine microbiome, to which they are beneficial, and one of the most abundant taxa in wine fermentation (Ohwofasa et al., 2023,

**Table 3**

Mass balance of ethanol and acetate in the different conditions tested. \* = calculated considering the acetate produced by EEO and the balance of acetate produced and consumed in chain elongation.

	Unit	WWL	WWL + inoc	RWL	RWL + inoc	gCOD/L			
						20	40	70	100
ETOH CONSUMED (OVERALL)	mMol	15.9	14.0	2.7	20.0	12.8	33.6	61.1	87.9
ETOH CONSUMED IN CHAIN ELONGATION	%	12.0	5.0	47.0	23.8	13.8	12.2	14.1	17.1
ETOH CONSUMED IN EEO	%	88.1	95.0	53.01	76.2	86.2	87.8	86.0	82.9
ACETATE PRODUCED IN THE TEST (MEASURED)	mMol	11.4	12.42	2.94	15.5	15.2	38.1	63.23	71.9
Acetate produced from ethanol*	%	115.5	103.4	19.8	85.1	65.6	71.3	79.8	98.7
Acetate produced from the substrates	%	0.0	0.0	80.2	14.9	34.4	28.7	20.2	1.4
ERROR IN THE MASS BALANCE	%	15.5	3.4	0.0	0.0	0.0	0.0	0.0	0.0

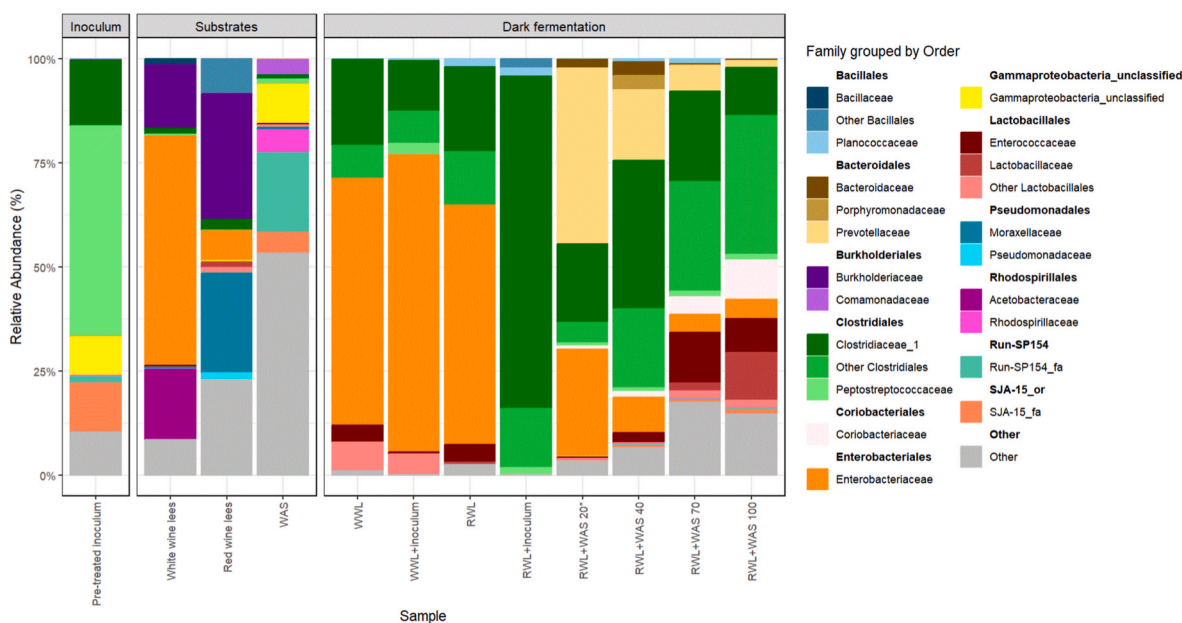


**Fig. 2.** Relative abundance of the bacterial community of the pre-treated inoculum and substrates at the beginning of the experiment and the acidogenic fermentation samples on day 7. The 12 most abundant orders and the two most abundant families for each order were represented. \* = on day 4.

**Table 4**

Ecological indices of the bacterial community of the pre-treated inoculum and substrates at the beginning of the experiment and the acidogenic fermentation samples on day 7. \* = on day 4.

	Richness	Shannon diversity	Simpson diversity	Pielou's evenness
<b>SUBSTRATES</b>				
Pre-treated inoculum	565	3.208	0.173	0.506
Red wine lees	60	3.228	0.070	0.788
White wine lees	231	2.687	0.214	0.494
WAS	820	5.486	0.011	0.818
<b>ACIDOGENIC FERMENTATION</b>				
WWL	80	2.012	0.259	0.459
WWL + inoc	89	1.979	0.328	0.441
RWL	67	1.892	0.324	0.450
RWL + inoc	103	2.346	0.233	0.506
RWL + WAS 20	392	2.942	0.161	0.493
RWL + WAS 40	567	4.134	0.038	0.652
RWL + WAS 70	453	4.175	0.033	0.683
RWL + WAS 100	433	3.915	0.051	0.645

and references therein). Only 4 families had a relative abundance >1% in white wine lees, representing 88.83% of the total: *Acetobacteraceae*, *Burkholderiaceae*, *Enterobacteriaceae*, and *Halomonadaceae*. In red wine lees, 5 families had a relative abundance >1%, representing 60.20% of the total: *Burkholderiaceae*, *Enterobacteriaceae*, *Micrococcaceae*,

*Moraxellaceae*, and *Staphylococcaceae*. All the identified genera were aerobic or facultatively anaerobic, coherently with the storage of WL in closed barrels in contact with air. After fermentation of WL without inoculum, these genera were not present at relative abundances >1%, except for *Klebsiella*. Instead, some indigenous facultative and strictly anaerobic bacteria became dominant (Table S3), which were probably selected during the anaerobic alcohol production in the winemaking process and allowed the anaerobic fermentation of WL without inoculation.

WAS had the highest richness (820), evenness (0.818), and Shannon's diversity (5.49) (Table 4), and it was composed by 88.79% of species with a relative abundance lower than 1% (Table S2). WAS served also as inoculum, and ecological indices show that the pretreatment successfully selected the spore-forming, H<sub>2</sub>-producing microorganisms. In fact, the richness of pre-treated inoculum was lower, showing that only the resistant microorganisms survived: *Eubacteriales* increased their relative abundance from 0.59 to 49.75% in WAS and pre-treated inoculum, respectively.

In the first test on WL, similar richness and diversity were observed in WWL and WWL + inoc, coherently with their comparable microbiome composition and fermentation performance (Table 4). RWL + inoc showed higher richness than RWL (103 vs 67, respectively), while diversity and evenness were comparable. This suggested that the low carboxylates production in RWL was due to the lack of some acidogenic bacteria added with the inoculum and already present in WWL, rather than to richness and diversity. In co-fermentation, richness and diversity

were higher with respect to the fermentation of WL alone due to WAS, a biologically active substrate (Table 4). For this reason, in co-fermentation only 45.6–49.7% of the taxa had relative abundance >1%, with respect to 76.4–92.8% of WL fermentation (Table S3). Ecological indices in co-fermentation at day 7 were similar among them, coherently with the product yields.

Regarding the microbiome composition, in all conditions the dominant families were *Clostridiaceae* (8.0–70.6%) and *Enterobacteriaceae* (3.5–61.0%). *Clostridiaceae* were ubiquitous, while *Enterobacteriaceae* were absent in RWL + inoc and were particularly enriched in WWL (57.4%), WWL + inoc, (61.0%) and RWL (54.8%), consistently with their high abundance in grape microbiome and wine fermentation (Ohwofasa et al., 2023, and references therein). Families of the *Lactobacillales* order were also present up to 15.20%, with higher relative abundances in co-fermentation at 70 and 100 gCOD/L, where caproate and heptanoate were detected, suggesting that some lactate could have been produced and used as electron donor. In the first test on WL, microbial communities were similar in WWL and WWL + inoc, as well as the fermentation products profile, except for some caproate (0.17 gCOD/L) detected only in WWL. Since *Caproiciproducens* (OTU 16, 97.78% similarity) was present in both conditions, the absence of caproate in WWL + inoc could be due to its lower butyrate concentration (0.20 vs 0.44 gCOD/L). This could be in turn due to the lower relative abundance of *Clostridiaceae* (11.02 vs 19.72%), a family including several chain-elongating species which could perform chain elongation of acetate to butyrate (section 3.4) (Candry and Ganigué, 2021, and references therein). In RWL, after the H<sub>2</sub> production phase (day 2), microbial communities were dominated by the H<sub>2</sub>-producer *Klebsiella* (81.6%) in RWL, where almost no carboxylates were detected, and by *Paraclostridium* (OTU 5) and *Clostridium* (OTU 7) (31.70 and 42.56%, respectively) in RWL + inoc, where 0.232 gCODprod/gbCOD were obtained. Therefore, it was hypothesized that *Klebsiella* lacks the ability to anaerobically oxidate ethanol to acetate, identified in *Clostridium* spp., thus explaining the lower acetate production (Tao et al., 2017; Wu et al., 2020). Microbiome composition could also explain the lower H<sub>2</sub> yield of WWL respect to RWL: in fact, the higher initial ethanol content in WWL fermentation (~7.4 g/L) could have lowered H<sub>2</sub> production by inhibiting *Klebsiella* and *Clostridiaceae* spp., which yield 2.07 and 2.81 mol H<sub>2</sub>/mol glucose, respectively, and favouring *Escherichia-Shigella*, which has lower yields of 1.44 mol H<sub>2</sub>/mol glucose but can tolerate ethanol concentrations up to 7.83 g/L (Lin et al., 2007; Niu et al., 2010; Seppälä et al., 2011; Wu et al., 2021).

In co-fermentation, a shift in microbial communities was observed with the increasing substrate concentrations. *Clostridiaceae*, *Coriobacteriaceae*, *Enterobacteriaceae*, *Enterococcaceae*, *Oscillospiraceae* and *Prevotellaceae* were always present, while *Lactobacillaceae* and *Family XIII* appeared from 40 gCOD/L. *Prevotella*, an acetate- and propionate-producing genus, decreased its relative abundance from 20 to 100 gCOD/L, (35.5–0.1%, respectively), coherently with its ethanol inhibition threshold of 6 g/L (Ma et al., 2022; Rui et al., 2019). At 70 and 100 gCOD/L, lactate-producers *Enterococcaceae*, *Lactobacillaceae*, and *Coriobacteriaceae* increased their relative abundance up to 9.55%, 8.92%, and 6.01%, respectively, suggesting that some lactate could have been produced and consumed as electron donor in chain elongation. This would be supported also by the progressive shift to lactate production at acetate concentrations higher than 100 mM observed by Noguera et al. (2022) at initial pH of 6, considering that in our tests acetate concentration increased from 89.4 to 93.8 mMol at day 4–142.0–162.8 mMol at day 7 at 70 and 100 gCOD/L, respectively. Coherently with the appearance of caproate, also the butyrate-producing *Eubacteriales Family XIII* was more abundant at 70 and 100 gCOD/L (6.86 and 15.85%, respectively) (Wylensek et al., 2020). Interestingly, the relative abundance of the putative chain-elongating *Clostridiaceae* and *Oscillospiraceae* families did not increase at 70 and 100 gCOD/L, even if an increase in their absolute abundance cannot be excluded. This suggested that in this case, chain elongation was triggered by the metabolic and community

shift to lactate production rather than by an increase in *Clostridiaceae* or *Oscillospiraceae*. It was reported that lactate- and ethanol-based chain elongation boosted each other, because the former produced the CO<sub>2</sub> needed for the growth of chain-elongating microorganisms (Wu et al., 2018). However, CO<sub>2</sub> was produced also at 20 and 40 gCOD/L, where caproate and heptanoate were not detected (Table 2), indicating that probably it was not a determining factor in the occurrence of chain elongation.

The Spearman's correlation calculated on the fermented samples mainly reflected the fact that products concentrations increased with substrate concentrations: in fact *Lactobacillaceae*, *Eubacteriales Family XIII* and *Coriobacteriaceae* had a significant positive correlation with acetate, butyrate, valerate, heptanoate, 1,3-propanediol and total carboxylates (Fig. S2). These families were present only in RWL + WAS, and their relative abundance increased with substrate concentrations. However, Spearman's correlation did not help identifying more precisely the role of each family or genus.

Finally, PCoA showed a clear clustering based on the type of substrates and fermented samples and metabolites profile obtained. According to the screeplot, the first 3 principal components (PCo) were considered, accounting for 53.9% of the variability of our dataset (Fig. 3A). After plotting each PCo against the other two, a similar clustering was observed, and therefore only PCo1 vs PCo2 was reported in Fig. 3B. PCo1 and PCo2 represented together 40.9% of the variability, with PCo1 separating RWL + WAS 40, 70, and 100 at day 7, and WAS and pretreated inoculum. PCo2 separated RWL from WWL and RWL 20 from RWL + inoc. RWL + WAS 20 stood alone, as expected since it was withdrawn on day 4. The notable distance between RWL 20 and RWL + inoc was coherent with the difference in their microbial communities and carboxylates production. RWL + inoc was located between RWL + WAS 20, with which it shared a similar carboxylates profile and

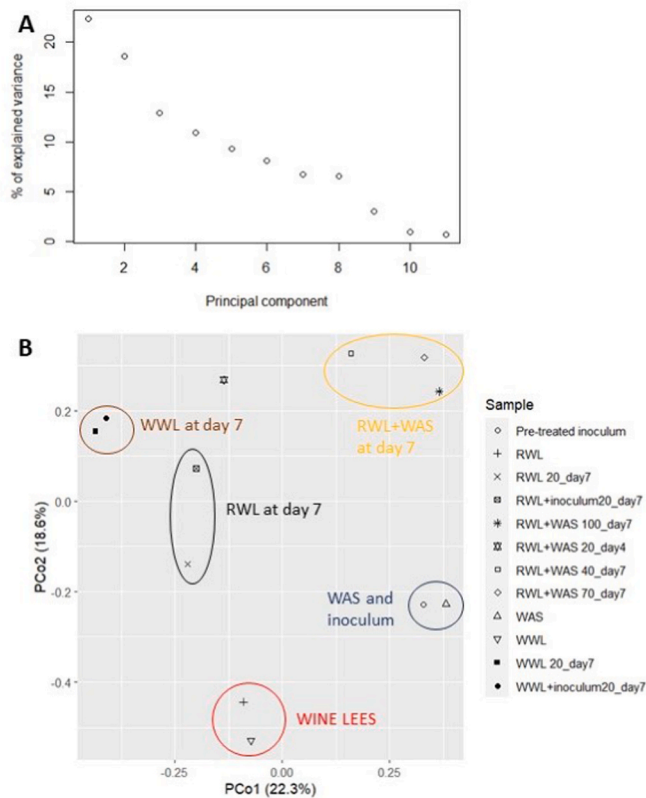


Fig. 3. Principal Component Analysis (PCoA) of the substrates and fermented samples. A) Screeplot reporting the percentage of variance explained by each principal component (PCo), showing that from PCo3 a lower amount of variance was explained and B) plot of PCo1 vs PCo2, showing samples clustering.

microbiome (*Clostridium perfringens*, *Clostridium prolinivorans/swellfuitianum*), and RWL 20, with which it shared a similar H<sub>2</sub> yield. Finally, the samples from co-fermentation were closer to WAS than WL, indicating that WAS mainly shaped their microbiomes. Almost all the environmental parameters were significant for explaining the samples distribution in the PCoA space, coherently with the difference in the nature of the samples analyzed.

#### 4. Conclusions

In conclusion, this study unlocked the potential of wine lees for high selective fermentative acetate production (57.5–72.3%) by the indigenous microbiome (WWL), by adding an external inoculum (RWL), or by co-fermentation with WAS. In co-fermentation, the increase in substrate concentration to 70 and 100 gCOD/L resulted in caproate (10.0–16.0%) and heptanoate (1.6–5.4%) production and in a microbiome enriched in lactate-producers up to 21.2%, suggesting the occurrence of a lactate-based chain elongation. Overall, this study represents a significant advancement towards the production of tailored effluents for bio-refinery process coupling, unlocking the major bottleneck represented by the poor metabolization of longer-chain carboxylates by microalgae and MECs.

#### CRedit authorship contribution statement

**Alice Lanfranchi:** Writing – review & editing, Writing – original draft, Visualization, Investigation, Formal analysis, Data curation, Conceptualization. **Jose Antonio Magdalena:** Supervision. **Cristina Cavinato:** Supervision, Funding acquisition, Conceptualization. **Eric Trably:** Writing – review & editing, Supervision, Resources, Funding acquisition, Conceptualization.

#### Declaration of competing interest

The authors declare that they have no known competing financial interests or personal relationships that could have appeared to influence the work reported in this paper.

#### Acknowledgments

Alice Lanfranchi would like to thank the Italian Ministry of Education and Merit for funding her PhD scholarship. Jose Antonio Magdalena would like to thank the Complutense University of Madrid for the financing of his contract at LBE-INRAE (France), with funds from the Ministry of Universities for the requalification of the Spanish University System for 2021–2023 (Modality 1. Margarita Salas), coming from the European Union-Next generation EU funding. This work was partially supported by DAIS- Ca' Foscari University of Venice within the IRIDE program. Analyses and experiments were performed at the Bio2E platform (<https://doi.org/10.5454/1.557234103446854E12>). The authors would like to thank Gaëlle Santa-Catalina for performing the biomolecular analyses. Margot Mahieux is gratefully acknowledged for her help with the nested barplot (Fig. 2).

#### Appendix A. Supplementary data

Supplementary data to this article can be found online at <https://doi.org/10.1016/j.jenvman.2024.123532>.

#### Data availability

Sequences are available in GenBank, under the accession number PRJNA1028514. Data will be made available upon request.

#### References

- Ahnert, M., Schalk, T., Brückner, H., Effenberger, J., Kuehn, V., Krebs, P., 2021. Organic matter parameters in WWTP – a critical review and recommendations for application in activated sludge modelling. *Water Sci. Technol.* <https://doi.org/10.2166/wst.2021.419>.
- Alibardi, L., Cossu, R., 2016. Effects of carbohydrate, protein and lipid content of organic waste on hydrogen production and fermentation products. *Waste Manag.* 47, 69–77. <https://doi.org/10.1016/j.wasman.2015.07.049>.
- Anderson, K., Jensen, H.G., 2018. How much government assistance do European wine producers receive? *World Scientific Handbook in Financial Economics Series 6*, 197–217. <https://doi.org/10.1017/jwe.2016.16>.
- Argun, H., Kargi, F., 2009. Effects of sludge pre-treatment method on bio-hydrogen production by dark fermentation of waste ground wheat. *Int. J. Hydrogen Energy* 34, 8543–8548. <https://doi.org/10.1016/j.ijhydene.2009.08.049>.
- Bardi, M.J., Vinardell, S., Astals, S., Koch, K., 2023. Opportunities and challenges of micronutrients supplementation and its bioavailability in anaerobic digestion: a critical review. *Renew. Sustain. Energy Rev.* <https://doi.org/10.1016/j.rser.2023.113689>.
- Bastidas-Oyanedel, J.R., Mohd-Zaki, Z., Zeng, R.J., Bernet, N., Pratt, S., Steyer, J.P., Batstone, D.J., 2012. Gas controlled hydrogen fermentation. *Bioresour. Technol.* 110, 503–509. <https://doi.org/10.1016/j.biortech.2012.01.122>.
- Bordiga, M., 2016. Valorization of wine making by-products. <https://doi.org/10.1201/b19423>.
- Bustamante, M.A., Moral, R., Paredes, C., Pérez-Espinosa, A., Moreno-Caselles, J., Pérez-Murcia, M.D., 2008. Agrochemical characterisation of the solid by-products and residues from the winery and distillery industry. *Waste Manag.* 28, 372–380. <https://doi.org/10.1016/j.wasman.2007.01.013>.
- Candry, P., Ganigué, R., 2021. Chain elongators, friends, and foes. *Curr. Opin. Biotechnol.* 67, 99–110. <https://doi.org/10.1016/j.copbio.2021.01.005>.
- Carmona-Martínez, A.A., Trably, E., Milferstedt, K., Lacroix, R., Etcheverry, L., Bernet, N., 2015. Long-term continuous production of H<sub>2</sub> in a microbial electrolysis cell (MEC) treating saline wastewater. *Water Res.* 81, 149–156. <https://doi.org/10.1016/j.watres.2015.05.041>.
- Carrillo-Reyes, J., Albarrán-Contreras, B.A., Buitrón, G., 2019. Influence of added nutrients and substrate concentration in biohydrogen production from winery wastewaters coupled to methane production. *Appl. Biochem. Biotechnol.* 187, 140–151. <https://doi.org/10.1007/s12010-018-2812-5>.
- Cheah, Y.K., Vidal-Antich, C., Dosta, J., Mata-Álvarez, J., 2019. Volatile fatty acid production from mesophilic acidogenic fermentation of organic fraction of municipal solid waste and food waste under acidic and alkaline pH. *Environ. Sci. Pollut. Res.* 26 (35), 35509–35522. <https://doi.org/10.1007/s11356-019-05394-6>.
- Chen, Y., Jiang, S., Yuan, H., Zhou, Q., Gu, G., 2007. Hydrolysis and acidification of waste activated sludge at different pHs. *Water Res.* 41, 683–689. <https://doi.org/10.1016/j.watres.2006.07.030>.
- Ciani, M., Comitini, F., Mannazzu, I., 2018. Fermentation. *Encyclopedia of Ecology* 310–321. <https://doi.org/10.1016/B978-0-12-409548-9.00693-X>.
- Da Ros, C., Cavinato, C., Pavan, P., Bolzonella, D., 2017. Mesophilic and thermophilic anaerobic co-digestion of winery wastewater sludge and wine lees: an integrated approach for sustainable wine production. *J. Environ. Manag.* 203, 745–752. <https://doi.org/10.1016/j.jenvman.2016.03.029>.
- Dauptain, K., Schneider, A., Noguera, M., Fontanille, P., Escudie, R., Carrere, H., Trably, E., 2021. Impact of microbial inoculum storage on dark fermentative H<sub>2</sub> production. *Bioresour. Technol.* 319, 124234. <https://doi.org/10.1016/j.biortech.2020.124234>.
- De Iseppi, A., Lomolino, G., Marangon, M., Curioni, A., 2020. Current and future strategies for wine yeast lees valorization. *Food Res. Int.* 137. <https://doi.org/10.1016/j.foodres.2020.109352>.
- Dessi, P., Romans-Casas, M., Perona-Vico, E., Tedesco, M., Hamelers, H.V.M., Bañeras, L., Dolores Balaguer, M., Puig, S., 2024. Membrane-based fermentation enables highly selective caproic acid production from wine lees. *Chem. Eng. J.* 154539. <https://doi.org/10.1016/j.cej.2024.154539>.
- Dreywood, R., 1946. Qualitative test for carbohydrate material. *Industrial & Engineering Chemistry Analytical Edition* 18, 499.
- Esteban-Gutiérrez, M., García-Aguirre, J., Irizar, I., Aymerich, E., 2018. From sewage sludge and agri-food waste to VFA: individual acid production potential and up-scaling. *Waste Manag.* 77, 203–212. <https://doi.org/10.1016/j.wasman.2018.05.027>.
- Eurostat, 2023. Sewage Sludge Production and Disposal. European Statistical Office, Luxembourg, 26<sup>th</sup> July 2023. [https://ec.europa.eu/eurostat/web/products-datasets/-/env\\_ww\\_spd](https://ec.europa.eu/eurostat/web/products-datasets/-/env_ww_spd). (Accessed 2 February 2024).
- Galanakis, C.M., 2017. *Handbook of Grape Processing By-Products-Sustainable Solutions*. Academic Press.
- Hallenbeck, P.C., 2009. Fermentative hydrogen production: principles, progress, and prognosis. *Int. J. Hydrogen Energy* 34, 7379–7389. <https://doi.org/10.1016/j.ijhydene.2008.12.080>.
- IPCC, 2023. SYNTHESIS REPORT OF THE IPCC SIXTH ASSESSMENT REPORT (AR6) Summary for Policymakers.
- Jankowska, E., Chwiałkowska, J., Stodolny, M., Oleskiewicz-Popiel, P., 2015. Effect of pH and retention time on volatile fatty acids production during mixed culture fermentation. *Bioresour. Technol.* 190, 274–280. <https://doi.org/10.1016/j.biortech.2015.04.096>.
- Jasko, J., Skripsts, E., Dubrovskis, V., 2012. BIOGAS PRODUCTION OF WINEMAKING WASTE IN ANAEROBIC FERMENTATION PROCESS.

- Kleerebezem, R., Van Loosdrecht, M.C.M., 2010. A generalized method for thermodynamic state analysis of environmental systems. *Crit. Rev. Environ. Sci. Technol.* 40, 1–54. <https://doi.org/10.1080/10643380802000974>.
- Kreuger, E., Nges, I., Björnsson, L., 2011. Ensiling of crops for biogas production: effects on methane yield and total solids determination. *Biotechnol. Biofuels* 4, 1–8. <https://doi.org/10.1186/1754-6834-4-44>.
- Kucek, L.A., Xu, J., Nguyen, M., Angenent, L.T., 2016. Waste conversion into n-caprylate and n-caproate: resource recovery from wine lees using anaerobic reactor microbiomes and in-line extraction. *Front. Microbiol.* 7. <https://doi.org/10.3389/fmicb.2016.01892>.
- Lacroux, J., Llamas, M., Dauptain, K., Avila, R., Steyer, J.P., van Lis, R., Trably, E., 2023. Dark fermentation and microalgae cultivation coupled systems: outlook and challenges. *Sci. Total Environ.* 865, 161136. <https://doi.org/10.1016/j.scitotenv.2022.161136>.
- Lin, P.Y., Whang, L.M., Wu, Y.R., Ren, W.J., Hsiao, C.J., Li, S.L., Chang, J.S., 2007. Biological hydrogen production of the genus *Clostridium*: Metabolic study and mathematical model simulation. *Int. J. Hydrogen Energy* 32 (12), 1728–1735. <https://doi.org/10.1016/j.ijhydene.2006.12.009>.
- Ma, H., Yu, Z., Wu, W., Fu, P., Xia, C., Shiung Lam, S., Boer Emilia, D., Wang, Q., Gao, M., 2022. Effects of ethanol addition on caproic acid production and rumen microorganism community structure from straw fermentation. *Fuel* 327, 125142. <https://doi.org/10.1016/j.fuel.2022.125142>.
- Magdalena, J.A., Pérez-Bernal, M.F., Bernet, N., Trably, E., 2023. Sequential dark fermentation and microbial electrolysis cells for hydrogen production: volatile fatty acids influence and energy considerations. *Bioresour. Technol.* 374, 128803. <https://doi.org/10.1016/j.biortech.2023.128803>.
- Marone, A., Ayala-Campos, O.R., Trably, E., Carmona-Martínez, A.A., Moscoviz, R., Latrille, E., Steyer, J.P., Alcaraz-Gonzalez, V., Bernet, N., 2017. Coupling dark fermentation and microbial electrolysis to enhance bio-hydrogen production from agro-industrial wastewaters and by-products in a bio-refinery framework. *Int. J. Hydrogen Energy* 42, 1609–1621. <https://doi.org/10.1016/j.ijhydene.2016.09.166>.
- Miron, Y., Zeeman, G., Van Lier, J.B., Lettinga, G., 2000. The role of sludge retention time in the hydrolysis and acidification of lipids, carbohydrates and proteins during digestion of primary sludge in CSTR systems. *Water Res.* 34, 1705–1713. [https://doi.org/10.1016/S0043-1354\(99\)00280-8](https://doi.org/10.1016/S0043-1354(99)00280-8).
- Niu, K., Zhang, X., Tan, W.S., Zhu, M.L., 2010. Characteristics of fermentative hydrogen production with *Klebsiella pneumoniae* ECU-15 isolated from anaerobic sewage sludge. *Int. J. Hydrogen Energy* 35 (1), 71–80. <https://doi.org/10.1016/j.ijhydene.2009.10.071>.
- Noguer, M.C., Escudé, R., Bernet, N., Eric, T., 2022. Populational and metabolic shifts induced by acetate, butyrate and lactate in dark fermentation. *Int. J. Hydrogen Energy* 47, 28385–28398. <https://doi.org/10.1016/j.ijhydene.2022.06.163>.
- Ohwofasa, A., Dhami, M., Tian, B., Winefield, C., On, S.L.W., 2023. Environmental influences on microbial community development during organic pinot noir wine production in outdoor and indoor fermentation conditions. *Heliyon* 9, e15658. <https://doi.org/10.1016/j.heliyon.2023.e15658>.
- OIV, 2023. *State of the World Vine and Wine Sector in 2022*.
- Oliveira, M., Duarte, E., 2016. Integrated approach to winery waste: waste generation and data consolidation. *Front. Environ. Sci. Eng.* 10, 168–176. <https://doi.org/10.1007/s11783-014-0693-6>.
- Pérez-Bibbins, B., Torrado-Agrasar, A., Salgado, J.M., Oliveira, R.P. de S., Domínguez, J. M., 2015. Potential of lees from wine, beer and cider manufacturing as a source of economic nutrients: an overview. *Waste Manag.* 40, 72–81. <https://doi.org/10.1016/j.wasman.2015.03.009>.
- Ragauskas, A.J., Williams, C.K., Davison, B.H., Britovsek, G., Cairney, J., Eckert, C.A., Frederick, W.J., Hallett, J.P., Leak, D.J., Liotta, C.L., Mielenz, J.R., Murphy, R., Templar, R., Tschaplinski, T., 2006. The path forward for biofuels and biomaterials. *Science* 311, 484–489. <https://doi.org/10.1126/science.1114736>, 1979.
- Ramos-Suarez, M., Zhang, Y., Outram, V., 2021. Current perspectives on acidogenic fermentation to produce volatile fatty acids from waste. *Rev. Environ. Sci. Biotechnol.* <https://doi.org/10.1007/s11157-021-09566-0>.
- Raunkjer, K., Hvitved-Jacobsen, T., Nielsen, P.H., 1994. Measurement of pools of protein, carbohydrate and N D lipid in domestic. *Water Res.* 28, 251–262.
- Rebecchi, S., Pinelli, D., Bertin, L., Zama, F., Fava, F., Frascari, D., 2016. Volatile fatty acids recovery from the effluent of an acidogenic digestion process fed with grape pomace by adsorption on ion exchange resins. *Chem. Eng. J.* 306, 629–639. <https://doi.org/10.1016/j.cej.2016.07.101>.
- Roghair, M., Hoogstad, T., Strik, D.P.B.T.B., Plugge, C.M., Timmers, P.H.A., Weusthuis, R.A., Bruins, M.E., Buisman, C.J.N., 2018. Controlling ethanol use in chain elongation by CO<sub>2</sub> loading rate. *Environ. Sci. Technol.* 52, 1496–1506. <https://doi.org/10.1021/acs.est.7b04904>.
- Roslan, E., Magdalena, J.A., Mohamed, H., Akhbar, A., Shamsuddin, A.H., Carrere, H., Trably, E., 2023. Lactic acid fermentation of food waste as storage method prior to biohydrogen production: effect of storage temperature on biohydrogen potential and microbial communities. *Bioresour. Technol.* 378, 128985. <https://doi.org/10.1016/j.biortech.2023.128985>.
- Rui, Y., Wan, P., Chen, G., Xie, M., Sun, Y., Zeng, X., Liu, Z., 2019. Simulated digestion and fermentation in vitro by human gut microbiota of intra- and extra-cellular polysaccharides from *Aspergillus cristatus*. *LWT* 116, 108508. <https://doi.org/10.1016/j.lwt.2019.108508>.
- Seppälä, J.J., Puhakka, J.A., Yli-Harja, O., Karp, M.T., Santala, V., 2011. Fermentative hydrogen production by *Clostridium butyricum* and *Escherichia coli* in pure and cocultures. *Int. J. Hydrogen Energy* 36 (17), 10701–10708. <https://doi.org/10.1016/j.ijhydene.2011.05.189>.
- Tao, Y., Wang, X., Li, X., Wei, N., Jin, H., Xu, Z., Tang, Q., Zhu, X., 2017. The functional potential and active populations of the pit mud microbiome for the production of Chinese strong-flavour liquor. *Microb. Biotechnol.* 10, 1603–1615. <https://doi.org/10.1111/1751-7915.12729>.
- Teunisse, G.M., 2022. *Fantastic-Nested Bar Plots for Phyloseq Data*.
- Trably, E., Paillet, F., Escudé, R., Bernet, N., Couhert Barrau, C., 2017. Procédé de contrôle d'un réacteur de fermentation sombre (FR patent No. 3071612B1). Institut National de la Propriété Industrielle. <https://patentimages.storage.googleapis.com/32/dc/c7/f62bfa3e816d90/FR3071612B1.pdf>.
- Turon, V., Trably, E., Fouilland, E., Steyer, J.P., 2016. Potentialities of dark fermentation effluents as substrates for microalgae growth: a review. *Process Biochem.* 51, 1843–1854. <https://doi.org/10.1016/j.procbio.2016.03.018>.
- Vital-Jacome, M.A., Buitrón, G., 2021. Thermophilic anaerobic digestion of winery effluents in a two-stage process and the effect of the feeding frequency on methane production. *Chemosphere* 272, 129865. <https://doi.org/10.1016/j.chemosphere.2021.129865>.
- Wu, Q., Guo, W., Bao, X., Meng, X., Yin, R., Du, J., Zheng, H., Feng, X., Luo, H., Ren, N., 2018. Upgrading liquor-making wastewater into medium chain fatty acid: insights into co-electron donors, key microflora, and energy harvest. *Water Res.* 145, 650–659. <https://doi.org/10.1016/j.watres.2018.08.046>.
- Wu, S.L., Luo, G., Sun, J., Wei, W., Song, L., Ni, B.J., 2021. Medium chain fatty acids production from anaerobic fermentation of waste activated sludge. *J. Clean. Prod.* 279, 123482. <https://doi.org/10.1016/j.jclepro.2020.123482>.
- Wu, S.L., Sun, J., Chen, X., Wei, W., Song, L., Dai, X., Ni, B.J., 2020. Unveiling the mechanisms of medium-chain fatty acid production from waste activated sludge alkaline fermentation liquor through physiological, thermodynamic and metagenomic investigations. *Water Res.* 169, 115218. <https://doi.org/10.1016/j.watres.2019.115218>.
- Wylensek, D., Hitch, T.C.A., Riedel, T., Afrizal, A., Kumar, N., Wortmann, E., Liu, T., Devendran, S., Lesker, T.R., Hernández, S.B., Heine, V., Buhl, E.M., M'D'Agostino, P., Cumbo, F., Fischöder, T., Wyszkon, M., Looft, T., Parreira, V.R., Abt, B., Doden, H. L., Ly, L., Alves, J.M.P., Reichlin, M., Flisikowski, K., Suarez, L.N., Neumann, A.P., Suen, G., de Wouters, T., Rohn, S., Lagkouvardos, I., Allen-Vercoe, E., Spröer, C., Bunk, B., Taverne-Thiele, A.J., Giesbers, M., Wells, J.M., Neuhaus, K., Schnieke, A., Cava, F., Segata, N., Elling, L., Strowig, T., Ridlon, J.M., Gulder, T.A.M., Overmann, J., Clavel, T., 2020. A collection of bacterial isolates from the pig intestine reveals functional and taxonomic diversity. *Nat. Commun.* 11. <https://doi.org/10.1038/s41467-020-19929-w>.
- Yamada, E.A., Sgarbieri, V.C., 2005. Yeast (*Saccharomyces cerevisiae*) protein concentrate: preparation, chemical composition, and nutritional and functional properties. *J. Agric. Food Chem.* 53, 3931–3936. <https://doi.org/10.1021/jf0400821>.